

Attractive Potential around a Thermionically Emitting Microparticle

G. L. Delzanno,^{1,2} G. Lapenta,^{1,3} and M. Rosenberg⁴

¹*Istituto Nazionale per la Fisica della Materia (INFN), Politecnico di Torino, Italy*

²*Burning Plasma Research Group, Dipartimento di Energetica, Politecnico di Torino, Italy*

³*Plasma Theory Group, Theoretical Division, Los Alamos National Laboratory, Los Alamos, New Mexico 87545, USA*

⁴*Department of Physics, University of San Diego, San Diego, California 92110, USA*

(Received 3 July 2003; revised manuscript received 17 November 2003; published 22 January 2004)

We present a simulation study of the charging of a dust grain immersed in a plasma, considering the effect of thermionic electron emission from the grain. It is shown that the orbit motion limited theory is no longer reliable when electron emission becomes large: screening can no longer be treated within the Debye-Huckel approach and an attractive potential well can form, leading to the possibility of attractive forces on other grains with the same polarity. We suggest to perform laboratory experiments where emitting dust grains could be used to create nonconventional dust crystals or macromolecules.

DOI: 10.1103/PhysRevLett.92.035002

PACS numbers: 52.27.Lw, 52.65.-y

Introduction.—The study of the charging of objects immersed in a plasma is a classic problem of plasma physics with many applications [1], ranging from space problems to dusty plasmas to probe the theory for plasma diagnostics. Recently, the link between condensed matter or high energy-density plasma and strongly coupled dusty plasmas [2] has renewed interest in the process of charging and shielding of dust in plasmas.

The interaction between a plasma and an object is due to the plasma particles that hit the object's surface and are captured. In the absence of other processes, the higher mobility of the electrons leads to more electron capture by the object, which tends to charge negatively. However, in certain conditions, other processes need to be considered. For example, if the object immersed in the plasma is sufficiently warm, a significant number of electrons can be emitted by the thermionic effect, altering the balance between electron and ion capture, reducing the negative charge on the object, or even reversing its sign. An example of this process is given by small objects entering Earth's atmosphere (meteoroids). Recent work has shown that the heating of the meteoroids, due to their interaction with the atmosphere, can produce a considerable thermionic emission which can lead to positively charged meteoroids [3].

In the present work, we will consider how electron emission changes the process of charging an object immersed in a plasma, considering self-consistently charge collection on the object and the screening by the surrounding plasma. We focus particularly on the process of thermionic emission, but the results also apply to similar cases of photoemission and secondary emission that create a current of electrons emitted by the object. Two primary conclusions are reached. First, the process of electron emission by the object reduces the charges as expected by the orbit motion limited (OML) theory [1]. However, the quantitative effect of the thermionic emission predicted by the OML theory is accurate only for small objects. We find that, for objects larger than the

Debye length, the OML becomes grossly inaccurate. Second, in the presence of thermionic emission when the object is charged positively, the screening potential develops an attractive well. In contrast with the typical monotonic behavior predicted by the Debye-Huckel theory, we observe a potential well due to the presence of an excess of electron charge trapped around the emitting object.

Looking at the literature, we have found experimental evidence that heated emissive probes can determine a nonmonotonic behavior of the plasma potential [4]. This is commonly called the virtual cathode, namely, a region of zero electric field associated with a local excess of negative charges. However, as far as we know, the importance of this mechanism on the charging process occurring in a dusty plasma and its implications have not yet been recognized. The consequences of this behavior of the shielding potential can be considerable since potential wells can provide regions of attraction for other objects with the same sign of charge. Although the present mechanism is not the only instance when particles of the same charge immersed in a plasma can attract each other (see [5,6], and references therein), the mechanism presented here can be tested experimentally. For example, photoemission could be used instead of thermionic emission in existing experiments. Such experiments would be best conducted in microgravity (e.g., on the Alpha space station) where other attractive mechanisms (e.g., wake field [5,6], ion flow alignment [7]) may be less important.

Charging in presence of thermionic emission.—We consider a spherical, isolated dust grain of radius a immersed in a neutral, unmagnetized plasma consisting of electrons and singly charged ions. The grain is stationary, located at $r = 0$. Ion and electron collisions with a neutral gas background are neglected. Electrons and ions have different masses m_e and m_i and temperatures T_e and T_i , respectively. The grain has a surface temperature T_d and can emit thermionic electrons (W being its work function). The characteristic lengths of the system are the electron Debye length λ_{De} , the ion Debye length λ_{Di} ,

and the linearized Debye length λ_{Dlin} , defined as $1/\lambda_{\text{Dlin}}^2 = 1/\lambda_{\text{De}}^2 + 1/\lambda_{\text{Di}}^2$.

In the simplest model, neglecting any emissions from the dust particle surface, the grain is charged by the surrounding plasma (primary charging). Initially, electrons are more mobile than ions and charge the grain negatively by hitting its surface. Hence, the grain acquires a negative potential and creates an electric field that repels electrons and attracts ions. A dynamical equilibrium is eventually reached when the electron current to the dust is equal to the ion current. The OML theory [1] provides a description of the mechanism and gives the floating potential on the dust, $\phi(a)$, as a function of the plasma properties. Once $\phi(a)$ is known, the electric charge on the dust is determined by $Q_{\text{OML}} = 4\pi\epsilon_0 a(1 + a/\lambda_{\text{Dlin}})\phi(a)$ if one considers a Debye-Huckel potential around the dust with screening length given by λ_{Dlin} . Indeed, the OML theory is a good approximation for thick sheaths where $a \ll \lambda_D$, but breaks down for $a \gg \lambda_D$ [8,9].

The presence of electron emission from the dust (either photoelectric or thermionic) affects crucially the potential distribution around the dust. In this Letter we focus on thermionic emission. The starting point for a theoretical analysis of the thermionic current is the Sommerfeld model of a metal where the energy states are uniformly distributed and the free electrons have a Fermi distribution of probability to occupy a certain energy state. We have to distinguish between positively and negatively charged dust grains. In fact, when the dust grain is negatively charged, any electron with energy $1/2m_e v_r^2 > \psi$ (ψ being the minimum energy required to overcome the surface barrier) will be emitted, leading to the following thermionic current [10]:

$$I_{\text{th}} = \frac{16\pi^2 a^2 e m_e k^2 T_d^2}{h^3} \exp\left(-\frac{W}{kT_d}\right), \quad (1)$$

known as the Richardson-Dushman expression. When the grain is positively charged, the situation is slightly different as the electrons have to overcome the floating potential as well as the surface barrier. The thermionic current for a positively charged grain is [10]

$$I_{\text{th}} = \frac{16\pi^2 a^2 e m_e k^2 T_d^2}{h^3} \left(1 + \frac{e\phi(a)}{kT_d}\right) \exp\left(-\frac{W + e\phi(a)}{kT_d}\right). \quad (2)$$

When thermionic emission is added to the OML framework, the equilibrium floating potential is established by balancing the ion and electron currents from the surrounding plasma with the thermionic current emitted by the dust.

Simulation method.—To study the charging of a thermionically emitting dust particle, we have developed a particle-in-cell (PIC) code [11] for a spherical plasma with the stationary grain at the center and an outer radius R . The problem under investigation requires special boundary conditions. At the outer boundary some par-

ticles leave the system while others must be injected to represent an infinite plasma medium outside the simulation domain. The algorithm used to inject the particles is the same widely used in the literature [11]. At the inner boundary, the plasma particles reaching the grain surface are removed from the simulation and their charge is accumulated to the central dust grain, affecting its floating potential. The same injection method used for the outer boundary can be applied also to the thermionic emission at the inner boundary, but uses the dust temperature and not the plasma electron temperature to evaluate the distribution function of the emitted electrons. In PIC simulations, the emitted electrons are followed accurately and the electrons that cannot overcome the dust attraction return to the dust; it follows that the emission current must always be computed with Eq. (1), to avoid counting the retarding potential twice.

We have chosen the parameters of the system according to typical experimental conditions. In particular, we consider a Maxwellian plasma with electron temperature $T_e = 1$ eV, ion temperature $T_i = 0.2$ eV ($T_e/T_i = 5$), and an outer radius of the system $R = 500 \mu\text{m}$. Moreover, the plasma far away from the dust grain is Maxwellian at rest, with density $n_\infty = 6 \times 10^{15}$ part/m³. These parameters correspond to the electron Debye length $\lambda_{\text{De}} = 96.0 \mu\text{m}$, the ion Debye length $\lambda_{\text{Di}} = 42.9 \mu\text{m}$, and the electron plasma frequency $\omega_{\text{pe}} = 4.37 \times 10^9 \text{ s}^{-1}$. The linearized Debye length is $\lambda_{\text{Dlin}} = 39.1 \mu\text{m}$. The electron mass is chosen with its physical value, but the ion mass is only 100 times larger. This unphysical choice is common in the literature and is required to keep the cost of the simulation manageable. All the simulations are made with an initial number of particles, $N_e = N_i = 200\,000$, located on a uniform computational grid with $N_g = 200$ cells. The time step is chosen to satisfy the Courant-Friedrichs-Lewy condition, $\Delta t = 10^{-11}$ s. The radial position and two velocity components (radial and tangential) are stored for each particle during the simulation.

In the simulations, we start from a uniform Maxwellian plasma and let the system relax self-consistently until the charge on the dust grain and the shielding potential around it reach a steady state. At equilibrium, the dust charge fluctuates due to collection of plasma particles and we consider the mean value defined as an average over a time interval of $70\omega_{\text{pe}}^{-1}$ s, which is a sufficiently large multiple of the dust charging time to provide a filter of the high frequency fluctuations. Hereafter, “time average” will imply an average over the last $70\omega_{\text{pe}}^{-1}$ of the simulation, when the steady state is fully reached.

Note that all the results presented in the paper are obtained in the absence of collisions between plasma particles and neutrals. Thus our results should be reliable when the mean free path for collisions, λ_{coll} , is much greater than the electron Debye length, λ_{De} . This requirement is well met, for example, for weakly ionized plasmas: a glow discharge with pressure $p \sim 10$ mtorr, degree of ionization $\chi \sim 10^{-5}$, density of neutrals

$n_g \sim 10^{20} \text{ m}^{-3}$, plasma density $n \sim 10^{15} \text{ m}^{-3}$ leads to $\lambda_{\text{coll}}/\lambda_{\text{De}} \sim 65$.

Results.—To validate our simulation tool, we consider first the charging of a dust particle in the absence of any emission. We consider a dust of radius $a = 10 \mu\text{m}$. Since $a/\lambda_{\text{Dlin}} \approx 0.2$, the OML theory should be a good approximation and we expect our code to agree with theoretical predictions. This is indeed true; the time average floating charge is $Q_d = -1.54 \times 10^{-15} \text{ C}$, while the one predicted by the OML theory is $Q_{\text{OML}} = -1.64 \times 10^{-15} \text{ C}$. The relative difference is defined as $|Q_d - Q_{\text{OML}}|/\max(Q_d, Q_{\text{OML}}) = 6\%$. At dynamical equilibrium, the floating potential is $\phi_d = -1.1386 \text{ V}$, in good agreement with the one given by the OML theory, $\phi_{\text{OML}} = -1.1776 \text{ V}$ (relative difference 3%). Furthermore, the shielding potential follows closely the Debye-Huckel expression with a screening length equal to the linearized Debye length λ_{Dlin} .

We have also considered the primary charging mechanism for a dust of radius $a = 80 \mu\text{m}$. Since $a/\lambda_{\text{Dlin}} \approx 2$, we expect the OML theory to be unreliable. In fact, our code gives $Q_d = -2.04 \times 10^{-14} \text{ C}$ while $Q_{\text{OML}} = -3.19 \times 10^{-14} \text{ C}$ with a relative difference of 36%. On the other hand, the value of the floating charge defined by $Q_{\text{De}} = 4\pi\epsilon_0 a(1 + a/\lambda_{\text{De}})\phi(a)$ is a good estimate of Q_d ($Q_{\text{De}} = -1.92 \times 10^{-14} \text{ C}$). This is a consequence of the fact that when the dust radius grows, the screening length is determined by the electrons [9]. The profile of the time average shielding potential follows the Debye-Huckel expression but now with a screening length equal to the electron Debye length λ_{De} , as predicted in Ref. [9]. The time average floating potential obtained by the simulation is $\phi_d = -1.2044 \text{ V}$ and the relative difference with respect to $\phi_{\text{OML}} = -1.1776 \text{ V}$ is 2%. Thus, the OML theory gives a good estimate also when $a/\lambda_{\text{Dlin}} \approx 2$, provided that the screening length is determined by the electrons. The value of ϕ_d in the present case is more negative than in the case of $a = 10 \mu\text{m}$ due to the development of an absorption barrier that diminishes the ion current to the dust. Furthermore, the sheath is wider, of the order of several linearized Debye lengths. In summary, our code has confirmed all the theoretical predictions from the OML theory regarding nonemitting dust particles.

Next, we include thermionic emissions. We consider a dust at $T_d = 0.1 \text{ eV}$ and with work function $W = 2.2 \text{ eV}$ (representative of some metallic oxides). These parameters lead to a positively charged grain. We have performed a number of simulations varying the dust radius a . Here we focus on the case $a = 80 \mu\text{m}$ to point out the most relevant aspects of the role of thermionic emission in the charging mechanism. The dynamical equilibrium is reached in approximately two electron plasma periods, being determined essentially by the electron and thermionic currents. (The ion dynamics is relevant on a longer time scale, creating the nonmonotonic behavior of the ion density explained below.) The equilibrium charge is $Q_d = 8.51 \times 10^{-15} \text{ C}$, where the OML theory predicts $Q_{\text{OML}} =$

$5.17 \times 10^{-15} \text{ C}$ [based on expression (2) and λ_{Dlin}] or $Q_{\text{De}} = 3.12 \times 10^{-15} \text{ C}$ [based on expression (2) and λ_{De}]. However, when the thermionic effect is taken into account a comparison of the floating charge of the simulation and of the OML theory is no longer correct. In fact, the numerical factor that defines the floating charge from the floating potential depends on the potential distribution around the dust which, when thermionic emission is present, is not well represented by the Debye-Huckel potential (either with λ_{Dlin} or λ_{De}). Focusing on the floating potential, we find $\phi_d = 0.1016 \text{ V}$ while $\phi_{\text{OML}} = 0.1911 \text{ V}$. Interestingly, when the thermionic effect is present, the OML theory does not produce an accurate estimate of the charging mechanism of large grains (also in cases when, in the absence of thermionic emission, its predictions are acceptable). Moreover, we have checked that, for small objects, the OML theory is still reliable when electron emission is included.

Figure 1(left panel) shows the shielding potential at five different times of the simulation. A potential well is present. The presence of such a well is of considerable interest since it can lead to attractive forces on another dust particle, even when it has the same charge. In the right panel of Fig. 1 one can see the time average shielding potential (solid line) and the potential well is clearly visible. We have also shown the time average shielding potential obtained by two simulations with $T_d = 0.01 \text{ eV}$ (dotted line) and $T_d = 0.2 \text{ eV}$ (dash-dotted line).

Discussion.—How can a potential well form around the dust? The explanation comes from the comparison with the case of the absence of thermionic emission.

In the presence of sufficient thermionic emission (which is the case considered above) the dust is positively charged. The resulting electric field attracts electrons and repels ions. As a consequence, the electrons emitted from the dust are slowed down in a region very close to the dust. The more energetic electrons can escape and contribute to the thermionic current emitted from the dust but the rest of the thermionic electrons form an electron cloud. The electron cloud determines an

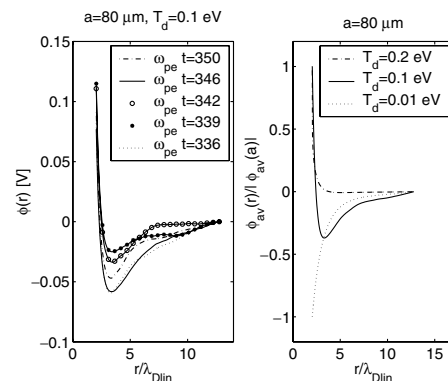


FIG. 1. Thermionic emission. Shielding potential $\phi(r)$ at different times (left panel) and time average shielding potential (right panel) as a function of the dust temperature.

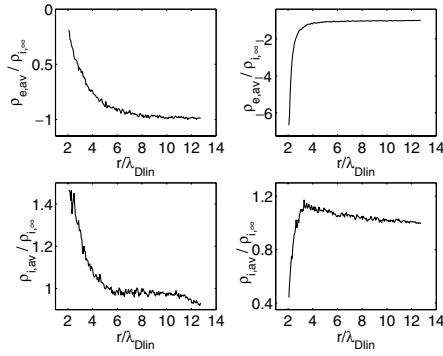


FIG. 2. Time average normalized electron and ion densities ρ_e and ρ_i for $a = 80 \mu\text{m}$: primary charging (left panels) and thermionic emission (right panels).

excess of negative charge and leads to an (equilibrium) potential well.

To support this explanation, Fig. 2 shows a comparison of the time average ion and electron density for the case with only primary charging (two left panels) and with thermionic emission (two right panels). The densities are normalized with respect to the unperturbed ion density, $\rho_{i,\infty}$. For the primary charging case, the densities are perturbed roughly to a distance of $4\lambda_{Dlin}$ from the dust grain; the electron density decreases while the ion density increases towards the grain. The last result is due to spherical geometry and to the ion angular momentum [9]. In fact, there are many ions with high angular momentum that do not strike the grain, thus leading to an increment of ion density in the sheath with respect to the equilibrium value. Consider next the case with thermionic effect (right panels). The electron density increases close to the grain due both to thermionic emission and to the attractive potential on the dust. On the other hand, since the grain is positively charged, the ion density diminishes approaching it. It can be noticed that the ion density increases from the dust grain somewhat up to $4\lambda_{Dlin}$, reaches a maximum, and decreases to the value at rest. Clearly, Fig. 2 shows the excess of electrons needed for the formation of the attractive well observed above.

We have performed another simulation where we have kept the potential on the dust fixed at the same potential observed in the simulation described above, in the presence of thermionic emission. In the present case, we impose the dust potential and we are not allowing any thermionic emission: only the primary charging is in effect. Note that this simulation is actually a description of the well-known Langmuir probe used in experimental plasma diagnostics. For this case, Fig. 3 shows the potential distribution at different times (left panel) and the time average shielding potential (right panel). One can see that the time average potential around the dust is a decreasing monotonic function of radius and vanishes asymptotically. Clearly, this confirms that the excess of electrons seen in Fig. 2 depends on the thermionic electrons.

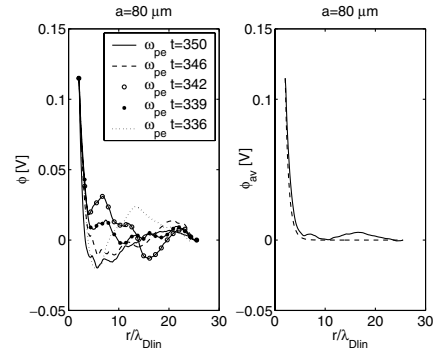


FIG. 3. Langmuir probe. Shielding potential $\phi(r)$ at different times (left panel) and time average shielding potential (right panel), for a dust particle with $a = 80 \mu\text{m}$. The Debye-Huckel potential with λ_{Dlin} (dashed line) is shown for comparison. The potential on the dust is held fixed at $\phi(a) = 0.115 \text{ V}$ and no thermionic electrons are emitted.

Finally, we have found the dust temperature critical for the well formation, as shown in Fig. 1 (right panel). When $T_d = 0.01 \text{ eV}$, the thermionic current is sufficiently small so that the grain is negatively charged and the shielding potential is an increasing monotonic function of radius (as for the primary charging case). When the dust temperature grows, for example, up to $T_d = 0.1 \text{ eV}$, an electron cloud forms around the dust and causes a potential well. However, if T_d is increased further (for example, $T_d = 0.2 \text{ eV}$), more thermionic electrons have enough kinetic energy to escape the dust attraction. At this high dust temperature, the local excess of electrons is reduced, the potential well disappears, and the shielding potential becomes a monotonically decreasing function of radius.

This work was partially supported by the IGPP-LANL Grant No. 03-1217 and by DOE Grant No. DEFG03-97ER54444. G.L.D. thanks Gianfranco Sorasio for many stimulating discussions and for his suggestions.

- [1] P. K. Shukla and A. Mamun, *Introduction to Dusty Plasma Physics* (IOP Publishing, London, 2002).
- [2] H. Thomas and G. E. Morfill, *Nature (London)* **379**, 806 (1996).
- [3] G. Sorasio, D. A. Mendis, and M. Rosenberg, *Planet. Space Sci.* **49**, 1257 (2001).
- [4] T. Intrator, M. H. Cho, E. Y. Wang, N. Hershkowitz, D. Diebold, and J. DeKock, *J. Appl. Phys.* **64**, 2927 (1988).
- [5] M. Nambu, S. V. Vladimirov, and P. K. Shukla, *Phys. Lett. A* **203**, 40 (1995).
- [6] P. K. Shukla and N. N. Rao, *Phys. Plasmas* **3**, 1770 (1996).
- [7] G. Lapenta, *Phys. Rev. E* **66**, 026409 (2002).
- [8] G. Lapenta, *Phys. Plasmas* **6**, 1442 (1999).
- [9] J. E. Daugherty, R. K. Porteous, M. D. Kilgore, and D. B. Graves, *J. Appl. Phys.* **72**, 3934 (1992).
- [10] M. Sodha and S. Guha, *Adv. Plasma Phys.* **4**, 219 (1971).
- [11] C. K. Birdsall and A. B. Langdon, *Plasma Physics Via Computer Simulation* (Adam Hilger, Bristol, 1991), p. 405.